

# Model for Nonlinear Transient Burning of Hydrazinium Nitroformate

Jeroen Louwers\* and Guy M. H. J. L. Gadiot†  
TNO Prins Maurits Laboratory, 2280 AA Rijswijk, The Netherlands

Transient burning of solid propellants is a topic that still contains a large number of questions. The transient burning of neat hydrazinium nitroformate is calculated within the quasi-steady gas-phase, homogeneous one-dimensional condensed phase approach. We focus on the effect of the condensed phase on the transient burning of solid propellants by showing the effect of temperature-dependent thermal properties, phase transitions, and chemical reactions in the solid phase. By solving the governing equations numerically, the nonlinear effects are conserved.

## Nomenclature

$A$	= preexponential factor, $s^{-1}$ , m/s
$c$	= specific heat, J/kg·K
$E$	= activation energy, J/mol
$k$	= thermal conductivity, W/m·K
$n$	= integer 0, 1, 2, . . .
$p$	= pressure, Pa
$Q$	= heat release, J/kg
$R$	= universal gas constant, J/mol·K
$R_p$	= pressure-driven response function
$r_b$	= propellant regression rate, m/s
$T$	= temperature, K
$t$	= time, s
$x$	= space coordinate, m
$\alpha$	= thermal diffusivity, $m^2/s$
$\epsilon$	= heat release rate, W/m <sup>3</sup>
$\rho$	= density, kg/m <sup>3</sup>
$\tau$	= nondimensional time

## Subscripts and Superscripts

$c$	= condensed phase
$f$	= flame
$g$	= gas phase
$m$	= melting of hydrazinium nitroformate
$s$	= surface
0	= initial
—	= on the negative side of
+	= on the positive side of
ref	= reference value
—	= steady-state value

## I. Introduction

IN the past, a lot of effort has been put into the development of models for transient burning of solid propellants. With the exception of a few models, most models share the same basic assumptions, of which the most important are homogeneous propellant with constant thermal properties, quasi-steady gas phase (QSG), and disregard of solid-phase reactions. In most models the condensed-phase reactions are collapsed to the surface, i.e., quasi-steady condensed-phase reactions (QSC). Several researchers have suggested that the existing models could be improved by accounting for chemical reactions in the solid phase.<sup>1,2</sup> Zebrowski and Brewster<sup>3</sup> reported

a large effect of condensed-phase unsteadiness on the transient response of a propellant. They showed that breakdown of the quasi-steady (QS = QSG + QSC) assumption is likely to occur in the condensed phase before it occurs in the gas phase. Similar results were obtained from an extended model for the transient combustion of ammonium perchlorate (AP)-based composite propellants.<sup>4</sup> This model accounts for distributed condensed-phase reactions and relaxes the QSC approximation. In this work, the AP model is applied to calculate the transient combustion of neat hydrazinium nitroformate (HNF). HNF is a high-performance chlorine-free oxidizer, which regained interest recently.<sup>5</sup> Like AP, HNF has very temperature-dependent thermophysical properties. The model accounts for condensed-phase reactions, melting of the HNF, and nonconstant thermophysical properties. The effect of the introduction of these aspects on the pressure-coupled response function is shown. It is the intention of this work to show the effect of combining all of the physical effects just described. This is not restricted to condensed-phase reactions as in the work of Zebrowski and Brewster,<sup>3</sup> but also includes nonconstant thermophysical properties and phase changes.

## II. Description of the Model

Figure 1 shows the model considered. Deep in the propellant's solid phase, the propellant has its initial temperature  $T_0$ . Because of the conductive heating by the gas phase and chemical reactions in the solid phase, the temperature in the solid increases up to the surface temperature  $T_s$ . At the surface, gasification of the solid takes place. Above the surface, the decomposition products react, until the gases reach the flame temperature  $T_f$ .

When the condensed phase is assumed to move with the burning rate  $r_b$  to the right, the surface will remain at a fixed position ( $x = 0$ ). For this situation, the energy equation of the condensed phase is given by the following parabolic partial differential equation<sup>6</sup>:

$$c_c(T)\rho_c \left[ \frac{\partial T}{\partial t} + r_b \frac{\partial T}{\partial x} \right] = \frac{\partial}{\partial x} \left[ k_c(T) \frac{\partial T}{\partial x} \right] + Q_c \epsilon_c(T) \quad \text{for } -\infty < x < 0 \quad (1)$$

where  $c_c$  is the heat capacity of the condensed phase,  $\rho_c$  is the density of the condensed phase,  $k_c$  is the thermal conductivity of the propellant, and  $Q_c \epsilon_c$  is the heat release distribution due to chemical reactions in the solid phase. This equation is nonlinear because of the terms  $r_b \partial T / \partial x$ ,  $Q_c \epsilon_c(T)$ , and the temperature-dependent thermophysical properties  $c_c(T)$ , and  $k_c(T)$ . It has been observed that the density of the liquid HNF is slightly lower than that of solid HNF.<sup>7</sup> This probably is caused by the gaseous decomposition products in the melting layer. Because no accurate experimental data are available, the density is assumed to be constant throughout the whole condensed phase.

Received 4 February 1998; revision received 25 August 1998; accepted for publication 30 August 1998. Copyright © 1999 by Jeroen Louwers and Guy M. H. J. L. Gadiot. Published by the American Institute of Aeronautics and Astronautics, Inc., with permission.

\*Ph.D. Student, P.O. Box 45; louwers@pml.tno.nl. Member AIAA.

†Senior Propulsion Engineer, P.O. Box 45.

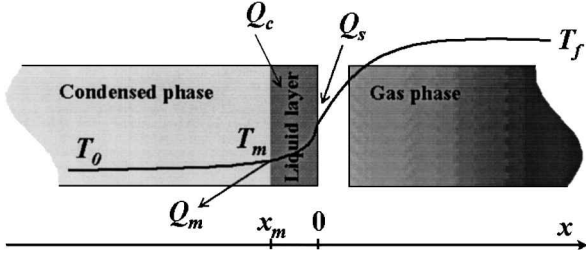


Fig. 1 Schematic of model for HNF combustion.

The regression rate is calculated from a zeroth-order Arrhenius law

$$r_b = A_s e^{-E_s/RT_s} \quad (2)$$

where  $E_s$  is the surface activation energy and  $T_s$  is the surface temperature.

On the cold boundary side,  $x \rightarrow -\infty$ , the boundary condition is given by

$$T(x \rightarrow -\infty, t) = T_0 \quad (3)$$

From an energy balance at the burning surface, the boundary condition at  $x = 0$  is found to be

$$\left[ k_c \frac{\partial T}{\partial x} \right]_{0^-} = q_{g,s} + r_b Q_s \quad (4)$$

where  $q_{g,s}$  is the heat flux from the gaseous phase to the surface of the propellant. At the surface, heat is released, which is described by the term  $Q_s$ . In most models, the surface heat release accounts for the total heat released in the condensed phase, which then is assumed to be collapsed at the surface. This allows for simple calculations because this term does not appear in the energy equation but in its boundary conditions. In the model presented, both the surface heat release  $Q_s$  and the condensed-phase heat release  $Q_c$  are considered.

The heat-release distribution function  $\epsilon_c$  may be assumed to be exponentially dependent on the temperature in the condensed phase

$$Q_c \epsilon_c(T) = A_c Q_c e^{-E_c/RT} \quad (5)$$

where  $E_c$  is the activation energy of the condensed-phase reactions. Because the decomposition in the solid phase is very small, it is assumed that  $\epsilon_c = 0$  in the solid phase. The preexponential factor  $A_c$  can be deduced from the normalization condition<sup>6</sup>

$$\int_{-\infty}^0 \epsilon_c(T(x)) dx = 1 \quad (6)$$

The decomposition activation energy of melted HNF was found to be 105 kJ/mol (Ref. 8). In case of surface-controlled kinetics, the surface activation energy is found from  $E_s = E_c/2$  (Ref. 9).

Several researchers have reported that combusting HNF shows a distinct melt layer at atmospheric combustion.<sup>7,10</sup> As the pressure is increased, this melt layer decreases in thickness. The position of the melting layer,  $x = x_m$ , is given by the condition

$$\left[ k_c(T) \frac{dT}{dx} \right]_{x=x_m^+} - \left[ k_c(T) \frac{dT}{dx} \right]_{x=x_m^-} = r_b \rho_c Q_m \quad (7)$$

where  $Q_m$  is the melting heat of HNF.

Experiments with embedded thermocouples show that the thermal diffusivity of HNF is not constant and is dependent on the temperature. The thermal diffusivity as a function of temperature was determined from measured thermocouple traces.<sup>7</sup> Figure 2 shows the thermal diffusivity used for the calculations presented. This temperature dependence of  $\alpha_c$  yields good agreement between experimental determined and calculated temperature profiles. The gradient between 350 and 370 K was introduced for computational stability.

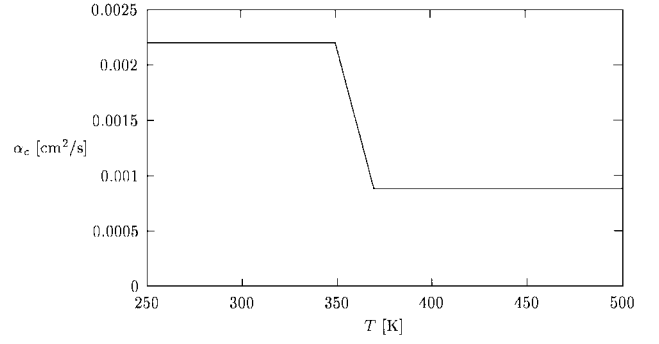


Fig. 2 Temperature-dependent thermal diffusivity of HNF used for the calculations.

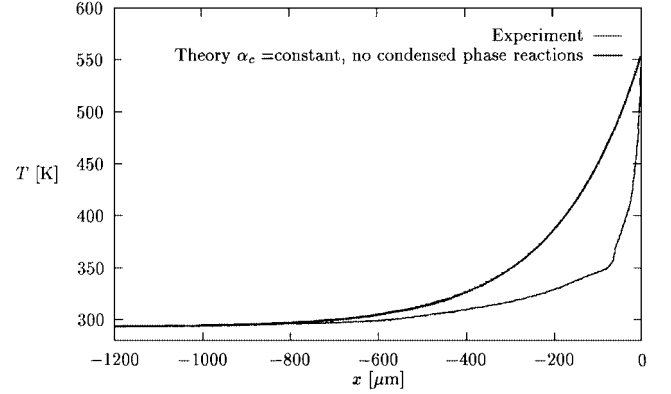


Fig. 3 Comparison between measured temperature profile and calculated profiles with constant (room temperature) thermophysical properties.

The reason for the sudden change in thermal diffusivity is unknown. Up to its melting point HNF has no phase changes.

Figure 3 compares a typical measured temperature profile in HNF combustion at ambient pressure with the theoretical temperature with constant thermal properties. It is clear that the constant-properties assumption is very crude and will yield different transient burning characteristics. It is the intention of this paper to show the effect of nonconstant thermal properties and condensed-phase reactions on the propellant's response function. The gas phase is considered to be quasi steady, which holds for low frequencies and low pressure. The heat feedback from the gaseous phase to the condensed phase ( $q_{g,s}$ ) is calculated using the  $\alpha\beta\gamma$  model with  $\alpha = 0$ ,  $\beta = 1$ , and  $\gamma = 0, 1, 2, \dots$  (Ref. 6). It is assumed further that this conductive heat transport is only pressure dependent. From these assumptions, it becomes clear that the gas phase is modeled very crudely; however, it is the objective of this study to analyze the effects of the processes in the condensed phase on the transient burning.

### III. Numerical Solution

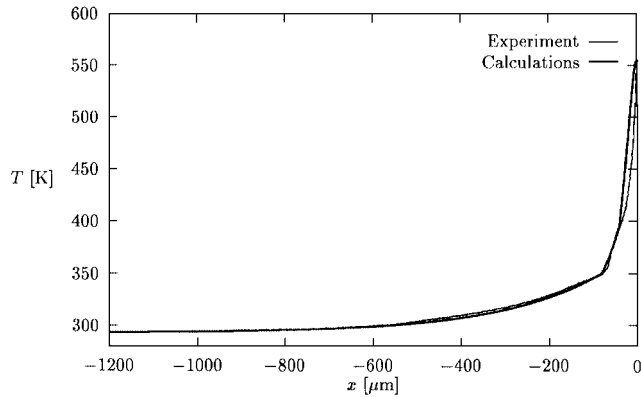
The equations are solved numerically by the use of an implicit finite difference method similar to that described in Ref. 11. In essence, this is a modified Crank–Nicholson method, with an improved stability of the time derivative by a weighted average of the points next to the point to be solved. Because of the steep gradients near the burning surface and the very slowly varying temperature near the cold end, a scale transformation was applied. This transformation enlarges intervals near the surface, and thus intervals far away from the surface are reduced.

The finite difference equations were implemented in a FORTRAN-77 computer program. This program first calculates the steady-state solution, which serves as a starting point for the transient calculations. This steady solution then is perturbed by a prescribed time-dependent (e.g., sinusoidal) pressure disturbance.

All calculations are performed at an ambient pressure of 0.1 MPa. The input data for the model are summarized in Table 1.

**Table 1** Model input data

Symbol	Value	Unit
$E_c$	105	kJ/mol
$Q_c + Q_s$	209	kJ/kg
$Q_m$	-161	kJ/kg
$T_f$	2766	K
$\rho_c$	1860	kg/m <sup>3</sup>
$r_b$	$0.922 \cdot (\bar{p}/p_0)^{0.828}$	mm/s
$T_s$	$553 \cdot (\bar{p}/p_0)^{0.079}$	K
$p_0$	0.1	MPa
$T_0$	293	K

**Fig. 4** Comparison between measured temperature profile and calculated profiles with nonconstant thermophysical properties and condensed-phase reactions.

## IV. Results

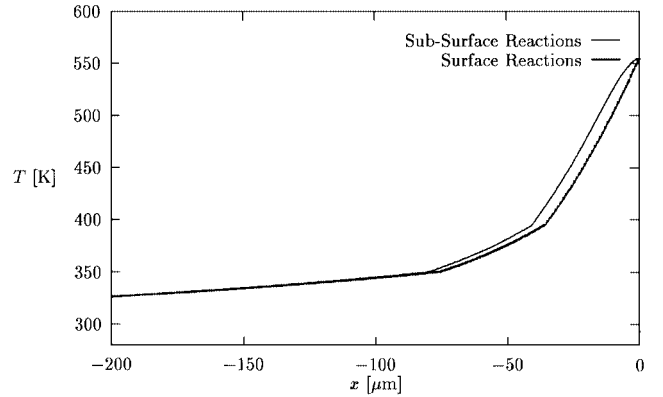
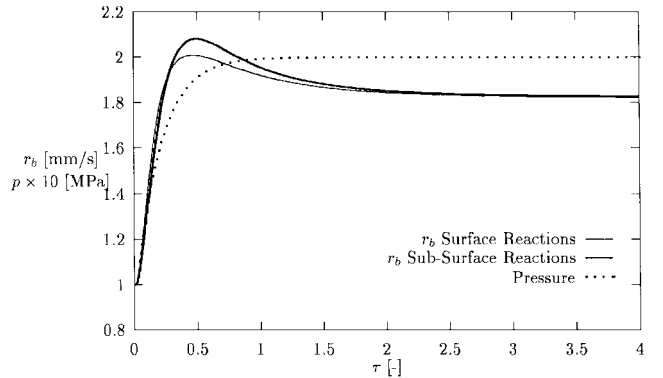
### A. Steady-State Burning

Figure 4 compares the calculated condensed-phase temperature profile with an experimentally determined profile. For this calculation, nonconstant thermophysical properties and condensed-phase reactions were used. Agreement with the experimental results is much better than for the constant properties from Fig. 3. Around the surface, there is still a deviation from the experimental results. Because of the limited amount of experimental data available and the steep gradient in this region, which limits the accuracy of the thermocouple experiments, no further attempts to improve the agreement were carried out. The difference in temperature profile between distributed condensed-phase reactions ( $Q_c \neq 0$ ) and surface-collapsed reactions ( $Q_s \neq 0$ ) is very small; see Fig. 5. This is because of the high activation energy, which results in a very small reaction layer very close to the surface. The effect of the spatial heat-release distribution during *transient* combustion is discussed in the next section.

### B. Transient Burning

To be able to calculate the transient burning of a solid rocket propellant, it is necessary that the propellant parameters be known accurately. The value of the total subsurface heat released by chemical reactions ( $Q_s + Q_c$ ) is a quantity that is difficult to measure. It was shown that the surface heat release  $Q_s$  is a very sensitive parameter for steady-state burning<sup>12</sup> as well as for transient burning, for which this sensitivity can be shown easily by linearized calculations. For these linearized calculations, the maximum of the pressure-driven response function is increased by a factor 2.5 when the surface heat release is increased from 100 to 125 cal/g (Ref. 6). It is shown here that, apart from the value of the total heat release in the condensed phase, the *distribution* of this heat release is also an important aspect. In all calculations, the total condensed-phase heat release ( $Q_s + Q_c$ ) is kept constant.

To verify the effect of the distribution of condensed-phase reactions on the transient burning of solid propellants, the response of the propellant during a pressurization was calculated. The calcu-

**Fig. 5** Calculated condensed-phase temperature profiles for surface and subsurface reactions.**Fig. 6** Calculated transient regression rates during an exponential pressure increase.

tions started from a steady state at  $t = 0$ , followed by an increase in pressure according to

$$p(\tau) = \bar{p} + \Delta p(1 - e^{-a\tau}) \quad (8)$$

where  $\tau$  is the nondimensional time defined as  $\tau = t/t_{\text{ref}} = t/(\alpha_c/r_{b,\text{ref}}^2)$ . For  $a > 1$ , the pressure rises faster than the propellant's characteristic time and essentially shows the propellant's response during a pressure step. Figure 6 shows the fluctuating surface temperature for a propellant with all of the chemical reactions collapsed to the surface ( $Q_s \neq 0$ ,  $Q_c = 0$ ), and a propellant with all chemical reactivity in the condensed phase ( $Q_s = 0$ ,  $Q_c \neq 0$ ). For these calculations,  $\bar{p} = \Delta p = 0.1$  MPa and  $a = 5$ . The total heat released by chemical reactions is assumed to be 50 cal/g (209 J/g). Compared to other propellants, this is relatively low, but this value matches the experimental observation of stable combustion even at ambient pressure and low surface temperature. As expected for high values of the activation energy, the response is very similar. The transient behavior can be attributed to the increase in burning rate during the increase in pressure. At higher burning rates, the thermal zone in the condensed phase is smaller. Because the temperature distribution is in its steady state at  $t = 0$ , the layer is too thick during the transition. Thus a preheated zone exists, which burns away fast (the maximum in the response).

Figure 7 shows a similar calculation for a very fast pressure drop from 0.5 to 0.1 MPa, with  $a = 50$ . It is seen that the propellant almost extinguishes because of the sudden drop in pressure (so-called depressurization extinguishment). The propellant with subsurface reactions recovers more slowly because of the time required to build up the condensed-phase thermal layer.

Figures 6 and 7 show that, even for high activation energies, a difference exists in a propellant's transient response to an external disturbance when calculations are carried out with surface-collapsed condensed-phase reactions or subsurface reactions. The response of the system is a function of the spectrum of the applied signal. The

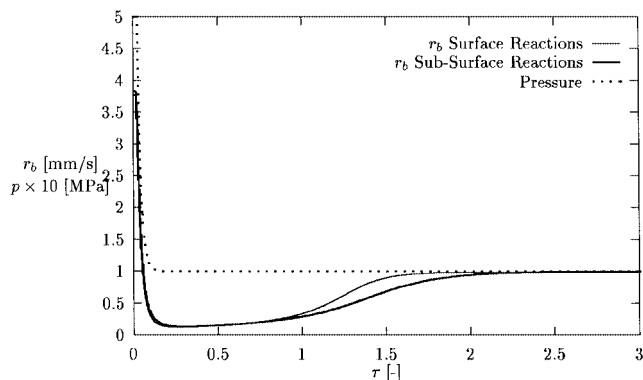


Fig. 7 Calculated transient regression rates during an exponential pressure drop.

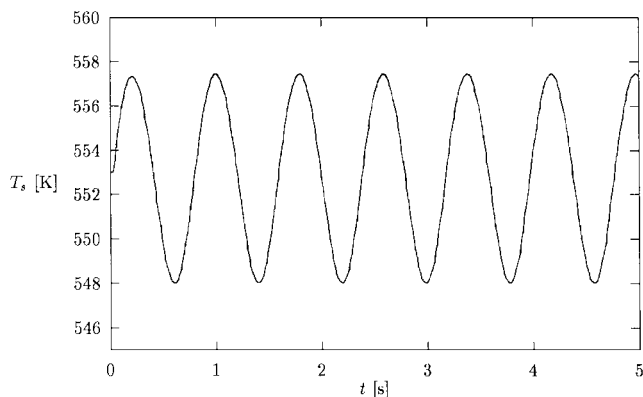


Fig. 8 Surface-temperature fluctuation during a sinusoidal pressure disturbance.

effect of the frequency on the response of the propellant is expressed by the response function. In the next section, these response functions are discussed. From these results, it will become clear that the response of the propellant to an external disturbance is frequency dependent and the response is therefore dependent on the frequency spectrum of the perturbing signal.

### C. Response Functions

From the transient calculations, the response function of the propellant can be calculated. The pressure-driven response function is computed by perturbing the steady state with a sinusoidal fluctuating pressure, with an amplitude of 10% of its mean value. After a few cycles, a situation of dynamic equilibrium develops. Figure 8 is an example of such a calculation. The relative change in burning rate  $r_b$  during this equilibrium divided by the relative change in pressure defines the pressure-coupled response function, according to

$$R_p = \frac{r'_b / \bar{r}_b}{p' / \bar{p}} \quad (9)$$

The effect of the temperature-dependent properties and condensed-phase reactions on the pressure-driven response functions is shown in Fig. 9. As seen from Figs. 3 and 4, the thermal-layer thickness of the analytical temperature profile is much larger than that of the other profiles obtained by nonconstant thermophysical properties. The thermal layer stores information of foregoing disturbances. Smaller zones have a higher resonance frequency, expressed by the shifting of the maximum of the response function to higher frequencies. Broad condensed-phase reaction zones have an opposite effect on the resonance frequency.

The effect of the melting of HNF is not only found in the thermal properties, but is coupled with it is the latent melting heat  $Q_m$ . The melting heat steepens the temperature profile further, increasing the resonance frequency. This is confirmed by the calculations of Fig. 10.

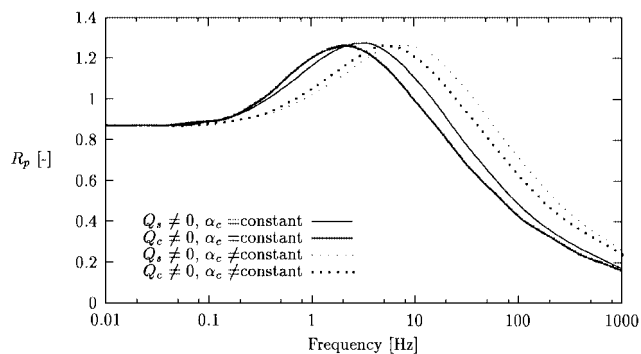


Fig. 9 Pressure-coupled response function for various situations (melting heat neglected).

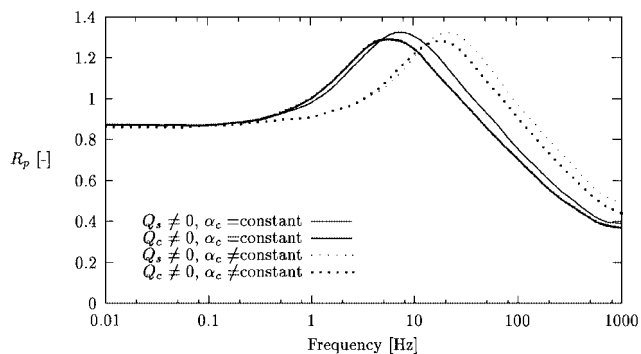


Fig. 10 Pressure-coupled response function for various situations (melting heat not neglected).

## V. Conclusions

The approximation of constant thermal properties is too crude to predict the response of a propellant accurately. The overall shift in the maximum of the response function is about an order of magnitude from the inert propellant with constant properties to the propellant with condensed-phase reactions and nonconstant thermal properties.

Phase changes in the condensed phase shift the maximum of the response function to higher frequencies.

Solid-phase reactions have a similar effect on the transient burning as the surface heat release. Subsurface reactions demonstrate a decrease in the resonance frequency for an increase in chemical reaction zone width.

### Note

At the time that this paper was written, no experimental transient HNF-data were available. In the meantime, Finlinson measured the laser-recoil response of HNF.<sup>13</sup> The model presented here was modified to include the external laser flux. The results of this modified model show good agreement with Finlinson's measurements.<sup>14</sup> Also, the source for the sudden decrease of thermal diffusivity has been identified. It turns out that cracks are formed during the combustion of pressed HNF pellets.<sup>14,15</sup> These cracks reduce the thermal conductivity.

## Acknowledgments

The authors would like to thank T. Parr and D. Hanson-Parr from Naval Air Warfare Center, China Lake, California, for the data provided and for helpful discussions.

## References

- Zarko, V. E., Simonenko, V. N., and Kiskin, A. B., "Radiation-Driven Transient Burning: Experimental Results," *Nonsteady Burning and Combustion Stability of Solid Propellants*, edited by L. Deluca, E. W. Price, and M. Summerfield, Progress in Astronautics and Aeronautics, Vol. 143, AIAA, Washington, DC, 1992, Chap. 10.

<sup>2</sup>Son, S. F., and Brewster, M. Q., "Unsteady Combustion of Homogeneous Energetic Solids Using the Laser-Recoil Method," *Combustion and Flame*, Vol. 100, Nos. 1, 2, 1995, pp. 283–291.

<sup>3</sup>Zebrowski, M. A., and Brewster, M. Q., "Theory of Unsteady Combustion of Solids: Investigation of Quasisteady Assumption," *Journal of Propulsion and Power*, Vol. 12, No. 3, 1996, pp. 564–573.

<sup>4</sup>Louwers, J., and Gadiot, G. M. H. J. L., "Nonlinear Transient Burning of Composite Propellants: Effect of Solid Phase Reactions," *Challenges in Propellants and Combustion 100 Years After Nobel*, edited by K. K. Kuo, Begell House, New York, 1997, pp. 1146–1156.

<sup>5</sup>Schöyer, H. F. R., Schnorhk, A. J., Korting, P. A. O. G., van Lit, P. J., Mul, J. M., Gadiot, G. M. H. J. L., and Meulenbrugge, J. J., "Development of Hydrazinium Nitroformate Based Solid Propellants," *Journal of Propulsion and Power*, Vol. 11, No. 4, 1995, pp. 856–869.

<sup>6</sup>DeLuca, L., "Theory of Nonsteady Burning and Combustion Stability by Flame Models," *Nonsteady Burning and Combustion Stability of Solid Propellants*, edited by L. Deluca, E. W. Price, and M. Summerfield, Progress in Astronautics and Aeronautics, Vol. 143, AIAA, Washington, DC, 1992, Chap. 14.

<sup>7</sup>Louwers, J., Parr, T., and Hanson-Parr, D., "HNF Combustion and Decomposition Experiments: UV-Absorption, Thermal Profile, PLIF," TNO Rept. PML 1997-C41, 1997.

<sup>8</sup>Koroban, V. A., Smirnova, T. I., Bashirova, T. N., and Svetlov, B. S., "Kinetics and Mechanism of the Thermal Decomposition of Hydrazine Trinitromethane," *Trudy Moskovskogo Khimiko-Tekhnologicheskogo Instituta*

imeni D. I. Mendeleeva, Vol. 104, 1979, pp. 38–44.

<sup>9</sup>Brill, T. B., "Multiphase Chemistry Considerations at the Surface of Burning Nitramine Monopropellants," *Journal of Propulsion and Power*, Vol. 11, No. 4, 1995, pp. 740–751.

<sup>10</sup>von Elbe, G., Friedman, R., Levy, J. B., and Adams, S. J., "Research on Combustion in Solid Rocket Propellants: Hydrazine Nitroform as a Propellant Ingredient," Atlantic Research Corp., TR DA-36-034-AMS-0091R, July 1964.

<sup>11</sup>Galfetti, L., Riva, G., and Bruno, C., "Numerical Computations of Solid-Propellant Nonsteady Burning in Open or Confined Volumes," *Nonsteady Burning and Combustion Stability of Solid Propellants*, edited by L. Deluca, E. W. Price, and M. Summerfield, Progress in Astronautics and Aeronautics, Vol. 143, AIAA, Washington, DC, 1992, Chap. 16.

<sup>12</sup>Hermance, C. E., "A Model of Composite Propellant Combustion Including Surface Heterogeneity and Heat Generation," *AIAA Journal*, Vol. 4, No. 9, 1966, pp. 1629–1637.

<sup>13</sup>Finlinson, J. C., "Laser Recoil Combustion Response of HNF Oxidizer from 1 to 6 ATM," AIAA Paper 97-3342, July 1997.

<sup>14</sup>Louwers, J., Gadiot, G. M. H. J. L., Versluis, M., Landman, A. J., vd Meer, Th. H., and Roekaerts, D., "Measurement of Steady and Non-Steady Regression Rates of Hydrazinium Nitroformate with Ultrasound," Politecnico di Milano, Milan, June 1998.

<sup>15</sup>Louwers, J., Gadiot, G. M. H. J. L., Versluis, M., Landman, A. J., vd Meer, Th. H., and Roekaerts, D., "Combustion of Hydrazinium Nitroformate Based Compositions," AIAA Paper 98-3385, July 1998.